ANISOTROPIC TOTAL VARIATION REGULARIZED LOW-RANK TENSOR COMPLETION BASED ON TENSOR NUCLEAR NORM FOR COLOR IMAGE INPAINTING

Fei Jiang[1], *Xiao-Yang Liu*[1,2], *Hongtao Lu*[1], *and Ruimin Shen*[1]

[1]Computer Science and Engineering, Shanghai Jiao Tong University, Shanghai, 200240, China
[1,2]Electrical Engineering,Columbia University, New York, NY10027, USA
jiangf@sjtu.edu.cn; xiaoyang@ee.columbia.edu; htlu@sjtu.edu.cn; rmshen@sjtu.edu.cn

ABSTRACT

In this paper, we propose a novel low-rank tensor completion (LRTC) model under the circulant algebra for color image inpainting, which simultaneously preserves the low-rank structures of images, and also explore the local smooth and piecewise priors of the images in the spatial domain. First, color images are naturally represented by 3-order tensors which preserve the intrinsic structures of color images. Second, we preserve the low-rank structures of these tensors with tensor nuclear norm, which can simultaneously exploit the correlations among the spatial and channel domains. Third, we integrate an anisotropic total variation into our low-rank tensor completion model, which preserve the local smooth and piecewise priors of color images. Then, an efficient alternating direction method of multipliers (ADMM) is proposed to solve the resulting optimization problem. Experimental results on eight widely used color images demonstrate the effectiveness and superiority of the proposed algorithm.

Index Terms – Low-rank tensor completion, tensor nuclear norm, anisotropic total variation.

1. INTRODUCTION

As a generalization of matrices and vectors, tensors are multi-dimensional array of numbers, which are natural form of multi-dimensional real world data. For example, color images and gray videos can be represented as 3-order tensors, where the three dimensions are height, width and color channel (temporal frame). Due to loss of information or unacceptable cost to acquire complete data, tensors used for real-world applications may contain missing values. Thus, completing the values for missing values, namely tensor completion problem, is of great importance for the real applications. Low-rank tensor completion (LRTC), which reveals the inherent structures of multi-dimensional data, has received considerable attentions, and been applied to many areas, such as computer vision [1], signal processing [2] and data mining [3].

Recent researches demonstrate the advantages of LRTC for the multi-dimensional data completion [4–9]. However, the rank of a tensor is not well-defined. Existing LRTC methods can be roughly broken down into three categories. The first category is based on CANDECOMP/PARAFAC (CP) [10] and the low rank of a tensor is defined as the minimum of rank 1 CP decomposition components. whereas, it is hard to determine, or even estimate, the rank of a tensor for real tensors [11, 12]. The second category is based on Tucker decomposition and the low-rank is commonly defined as the sum of nuclear norm (SNN) of unfolding matrices [4]. Due to the definition of Tucker decomposition, SNN does not exploit the correlations between different modes. Moreover, SNN tries to model the tensor in the matrix SVD-based vector space, which results in loss of optimality in the representation. The third category is based on the recently proposed t-SVD decomposition [13] and the low rank is defined as tensor nuclear norm (TNN)/ tensor tubal rank [6, 7]. Since t-SVD is based on an operator theoretic interpretation of 3-order tensors as linear operators on the space of oriented matrices, the tensor multi-rank and tubal rank can well characterize the inherent low-rank structure of a tensor while avoiding the loss of information inherent in matricization of the tensor [6]. In this paper, we focus on the tensor nuclear norm for the low-rank tensor completion.

Though the low-rank constraint is useful for the tensor completion, it is not efficient enough to exploit the local smooth and piecewise priors of the local structures in color images. As well known, color images, especially in the spatial domain, exhibits smooth and piecewise structures, due to objects or edges therein. Without considering such priors, the inpainting results may be unsatisfactory. Total variation (TV), a well-known norm to preserve piecewise smooth priors, has been successfully applied to image/video restorations [14]. In this paper, we propose to incorporate an anisotropic total variation into tensor recovery, which focuses on exploiting the local piecewise smooth structures in the spatial domain. The contributions are summarized as follows:

- We propose a novel low-rank tensor completion model, which simultaneously preserves the low-rank structures of images, but also exploit the local smooth and piecewise priors of the images in the spatial domain
- An efficient alternating direction method of multiplier-

s (ADMM) is proposed for solving the resulting optimization problems.

- Experimental results on 8 widely used color images demonstrated the effectiveness of our algorithms.

2. NOTATIONS AND PRELIMINARIES

We briefly introduce the notations and preliminaries throughout the paper. We use boldface capital letters for matrices, boldface lowercase letters for vectors, and lowercase for scalars. We denote a 3-order tensor by $\mathcal{X} \in \mathbb{R}^{n_1 \times n_2 \times n_3}$, its $ij\ell$-th element by $\mathcal{X}_{ij\ell}$, its frontal slice by $\mathcal{X}^{(\ell)} = \mathcal{X}(:,:,\ell)$, and the mode-$\ell$ unfolded matrix by $\mathbf{X}_{(\ell)}$, which is formed by arranging all the mode-ℓ fibers as columns of the matrix. The Fourier transform of $\mathcal{X}$ along the third dimension is denoted as $\widehat{\mathcal{X}} = \text{fft}(\mathcal{X}, [\,], 3)$. The ℓ_1 norm of tensor $\mathcal{X}$ is $\|\mathcal{X}\|_{\ell_1} = \sum_{i,j,\ell} |\mathcal{X}_{ij\ell}|$ and the Frobenius norm is $\|\mathcal{X}\|_F = \sqrt{\sum_{i,j,\ell} \mathcal{X}_{ij\ell}}$.

To construct our model based on tensor nuclear norm, it is necessary to introduce three block-based operators, i.e., $\text{bcirc}(\cdot)$, $\text{bvec}(\cdot)$, and $\text{bvfold}(\cdot)$, in advance. For $\mathcal{X} \in \mathbb{R}^{n_1 \times n_2 \times n_3}$,

$$\text{bcirc}(\mathcal{X}) := \begin{bmatrix} \mathcal{X}^{(1)} & \mathcal{X}^{(n_3)} & \cdots & \mathcal{X}^{(2)} \\ \mathcal{X}^{(2)} & \mathcal{X}^{(1)} & \cdots & \mathcal{X}^{(3)} \\ \vdots & \vdots & \ddots & \vdots \\ \mathcal{X}^{(n_3)} & \mathcal{X}^{(n_3-1)} & \cdots & \mathcal{X}^{(1)} \end{bmatrix}, \tag{1}$$

and the block vectorizing and its opposite operation

$$\text{bvec}(\mathcal{X}) := \begin{bmatrix} \mathcal{X}^{(1)} \\ \mathcal{X}^{(2)} \\ \vdots \\ \mathcal{X}^{(n_3)} \end{bmatrix}, \quad \text{bvfold}(\text{bvec}(\mathcal{X})) = \mathcal{X}, \tag{2}$$

where $\text{bcirc}(\mathcal{X})$ is of size $n_1 n_3 \times n_2 n_3$, and $\text{bvec}(\mathcal{X})$ is $n_1 n_3 \times n_2$. The t-product between two 3-order tensors can then be defined as follows [7, 13, 15].

Definition 1 *Let $\mathcal{A}$ be $n_1 \times r \times n_3$ and $\mathcal{B}$ be $r \times n_2 \times n_3$, the t-product $\mathcal{A} * \mathcal{B}$ is the order-3 tensor of size $n_1 \times n_2 \times n_3$, where*

$$\mathcal{X} = \mathcal{A} * \mathcal{B} = bvfold\left(bcirc(\mathcal{A}) \cdot bvec(\mathcal{B})\right), \tag{3}$$

where $\cdot$ denotes the standard matrix multiplication.

Definition 2 *Given a 3-order tensor $\mathcal{X} \in \mathbb{R}^{n_1 \times n_2 \times n_3}$, the t-SVD of $\mathcal{X}$ is given by*

$$\mathcal{X} = \mathcal{U} * \mathcal{S} * \mathcal{V}^\dagger, \tag{4}$$

where $\mathcal{U} \in \mathbb{R}^{n_1 \times r \times n_3}$ and $\mathcal{V} \in \mathbb{R}^{n_2 \times r \times n_3}$ are orthogonal tensors which satisfy $\mathcal{U}^\dagger * \mathcal{U} = \mathcal{I}$ and $\mathcal{V} * \mathcal{V}^\dagger = \mathcal{I}$. $\mathcal{I}$ is the identity tensor whose frontal slices are all zeros except the first one an identity matrix. $\mathcal{S} \in \mathbb{R}^{r \times r \times n_3}$ is a tensor whose frontal slices are diagonal matrices.

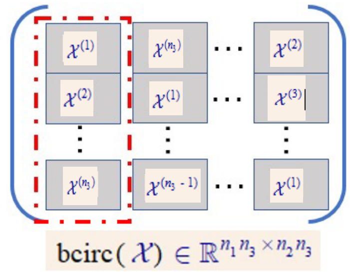

Fig. 1. Formulation of $\text{bcirc}(\mathcal{X})$. The dash block part is actually the unfolding matrix of $\mathcal{X}$ along the second mode $\mathbf{X}_{(2)}$.

Definition 3 *The tensor nuclear norm of $\mathcal{X} \in \mathbb{R}^{n_1 \times n_2 \times n_3}$ is defined as*

$$\|\mathcal{X}\|_{\circledast} := \sum_{\ell=1}^{n_3} \sum_{i=1}^{\min\{n_1,n_2\}} |\widehat{\mathcal{S}}_{ii\ell}|. \tag{5}$$

3. OUR MODEL

We first present the motivation for our model. Then we introduce our model followed by an efficient algorithm. After that, the computational complexity is analyzed.

3.1. Motivation

The task of tensor completion is to fill in the missing values of a tensor $\mathcal{X} \in \mathbb{R}^{n_1 \times n_2 \times n_3}$ under a given subset Ω. Since tensor data of high dimensional are usually underlying low-rank [16], tensor completion problem can be written as:

$$\min_{Z} \text{rank}_t(\mathcal{Z}), \;\; \text{s.t.} [\mathcal{Z}]_\Omega = [\mathcal{X}]_\Omega, \tag{6}$$

where rank_t is the rank of tensor $\mathcal{Z}$. However, minimizing $\text{rank}_t(\mathcal{Z})$ is complex. [15] and [7] replace $\text{rank}_t(\mathcal{Z})$ as the tensor nuclear norm (TNN), and achieve the state-of-the-art 3-order tensor completion results. Unlike SNN, TNN can well characterize the inherent low-rank structure of a tensor. Lemma 1 shows the equivalence of TNN in the real domain.

Lemma 1 *[6] Given $\mathcal{X} \in \mathbb{R}^{n_1 \times n_2 \times n_3}$, we have $\|\mathcal{X}\|_{\circledast} = \|bcirc(\mathcal{X})\|_*$.*

As shown in Figure 1 , the equivalent formulation of TNN, i.e., $\text{bcirc}(\mathcal{X})$, not only capture the low-rank structures of the unfolding matrix $\mathbf{X}_{(2)}$, but also captures the correlations between different modes. Therefore, TNN can characterize the inherent low-rank structures of a tensor without the loss of information inherent in matricization of the tensor.

On the other hand, many real world data show a local smooth and piecewise characteristic, such as the spatial dimensions of color images. The total variation (TV) norm is an appropriate choice to measure the piecewise smoothness of

Algorithm 1 Algorithms for our model.

Input: an incomplete tensor $\mathcal{X}$, iteration number k, parameters λ, $\{\rho_i\}_{i=1}^3$ and $\mu \in [1.1, 1.5]$,

1: Set randomly initialize $\{\mathbf{Q}_i, \mathbf{R}_i\}_{i=1}^3$, $\mathcal{M}$, $\mathcal{Z} = \mathcal{X}$

2: **for** $i = 1$ to k **do**

3: Update $\{\mathbf{Q}_i, \mathbf{R}_i\}_{i=1}^3$, $\mathcal{M}$, $\mathcal{Z} = \mathcal{X}$ as (12), (14), (15) and (17).

4: $\mathbf{\Lambda}_i = \mathbf{\Lambda}_i + \rho_1(\mathbf{Q}_i - \mathbf{F}_i\mathbf{R}_i)$, $\mathbf{\Phi}_i = \mathbf{\Phi}_i + \rho_2(\mathbf{R}_i - \mathbf{Z}_{(i)})$, $\Gamma = \Gamma + \rho_3(\mathcal{M} - \mathcal{Z})$, $\rho_i = \mu\rho_i, i = 1, 2, 3.$

5: **end for**

Output: $\mathcal{Z}$.

signals. An anisotropic total variation norm of a 3-order tensor $\mathcal{X} \in \mathbb{R}^{n_1 \times n_2 \times n_3}$ is used in our paper, with the following definition:

$$\|\mathcal{X}\|_{TV} = \sum_{i=1}^{3} \beta_i \|\mathbf{F}_i \mathbf{Z}_{(i)}\|_1, \tag{7}$$

where $\mathbf{F}_i$ is a $(n_i - 1)$-by-n_i matrix, where $[\mathbf{F}_i]_{i,i} = 1$, $[\mathbf{F}_i]_{i,i+1} = -1$, and the other entries are zeros. β_i is 0 or 1, which indicates whether we have a smooth and piecewise prior on the i-th mode of the recovered tensor. The setting of β_i is domain dependent. For example, when $\mathcal{X}$ represents a color image, we set $\beta_1 = \beta_2 = 1$ and $\beta_3 = 0$, due to the smooth and piecewise priors existing only in spatial domain.

3.2. TV Regularized Low-rank Tensor Completion

As previous discussion, we propose a novel low-rank completion model, which combines TNN and anisotopic total variation regularization, aiming at extracting intrinsic structures of visual data and exploiting the local smooth and piecewise priors, simultaneously.

Given an incomplete tensor $\mathcal{X} \in \mathbb{R}^{n_1 \times n_2 \times n_3}$ with Ω indicating the set of indices of observations, the tensor completion problem is defined as follows:

$$\begin{aligned} \min_{\mathcal{Z},\mathcal{A},\mathcal{B}} \quad & \lambda \sum_{i=1}^{p} \beta_i \|\mathbf{F}_i \mathbf{Z}_{(i)}\|_1 + \|\mathcal{Z}\|_{\circledast} \\ \text{s.t.} \quad & [\mathcal{Z}]_\Omega = [\mathcal{X}]_\Omega, \end{aligned} \tag{8}$$

where λ is a tunable parameter, balancing the TV regularization and the fidelity term.

By introducing three auxiliary variables, we rewrite (16) as the following equivalent minimization problem:

$$\begin{aligned} \min_{\mathcal{Z},\mathcal{A},\mathcal{B}} \quad & \lambda \sum_{i=1}^{p} \beta_i \|\mathbf{Q}_i\|_1 + \|\mathcal{M}\|_{\circledast} \\ \text{s.t.} \quad & \{\mathbf{Q}_i = \mathbf{F}_i\mathbf{R}_i, \mathbf{R}_i = \mathbf{Z}_{(i)}\}_{i=1}^3, \\ & \mathcal{M} = \mathcal{Z}, \\ & [\mathcal{Z}]_\Omega = [\mathcal{X}]_\Omega, \end{aligned} \tag{9}$$

Based on the augmented Lagrange methodology, problem (9) is changed into:

$$\begin{aligned} \mathcal{L} = & \sum_{i=1}^{3} \beta_i \cdot \left(\lambda \|\mathbf{Q}_i\|_1 + \frac{\rho_1}{2} \|\mathbf{Q}_i - \mathbf{F}_i\mathbf{R}_i + \frac{\mathbf{\Lambda}_i}{\rho_1}\|_F^2 \right) \\ & + \sum_{i=1}^{3} \beta_i \cdot \left(\frac{\rho_2}{2} \|\mathbf{R}_i - \mathbf{Z}_{(i)} + \frac{\mathbf{\Phi}_i}{\rho_2}\|_F^2 \right) \\ & + \|\mathcal{M}\|_{\circledast} + \frac{\rho_3}{2} \|\mathcal{M} - \mathcal{Z} + \frac{\Gamma}{\rho_3}\|_F^2, \end{aligned} \tag{10}$$

under the constraint $[\mathcal{Z}]_\Omega = [\mathcal{X}]_\Omega$. Matrices $\{\mathbf{\Lambda}_i\}_{i=1}^3$, $\{\mathbf{\Phi}_i\}_{i=1}^3$ and Γ are Lagrange multipliers.

Next, we derive the updating rules of $\{\mathbf{Q}_i\}_{i=1}^p$, $\{\mathbf{R}_i\}_{i=1}^p$, $\mathcal{M}$ and $\mathcal{Z}$ by fixing the other variables as follows: For $\mathbf{Q}_i$, if $\beta_i = 1$

$$\mathbf{Q}_i = \arg\min_{\mathbf{Q}_i} \lambda \|\mathbf{Q}_i\|_1 + \frac{\rho_1}{2} \|\mathbf{Q}_i - \mathbf{F}_i\mathbf{R}_i + \frac{\mathbf{\Lambda}_i}{\rho_1}\|_F^2, \tag{11}$$

which has a closed-form solution as:

$$\mathbf{Q}_i = \mathcal{P}_{\frac{\lambda}{\rho_1}} \left(\mathbf{F_i}\mathbf{R}_i - \frac{\mathbf{\Lambda}_i}{\rho_1} \right), \tag{12}$$

where $\mathcal{P}_\alpha(\cdot)$ is the elementwise shrinkage-thresholding operator, i.e. $\mathcal{P}_\alpha(\mathbf{X}) = \text{sign}(\mathbf{X}) \odot \max(\mathbf{X} - \alpha, 0)$, and $\text{sign}(\cdot)$ is the sign function, and $\odot$ is the element-wise multiplication.

Similarly, if $\beta_i = 1$,

$$\mathbf{R}_i = \arg\min_{\mathbf{R}_i} \rho_1 \|\mathbf{Q}_i - \mathbf{F}_i\mathbf{R}_i + \frac{\mathbf{\Lambda}_i}{\rho_1}\|_F^2 + \rho_2 \|\mathbf{R}_i - \mathbf{Z}_{(i)} + \frac{\mathbf{\Phi}_i}{\rho_2}\|_F^2, \tag{13}$$

and the closed-form solution is

$$\mathbf{R}_i = (\mathbf{F}_i^T\mathbf{F}_i + \rho_2\mathbf{I})^{-1}(\mathbf{F}_n^T\mathbf{\Lambda}_n + \rho_1\mathbf{F}_n^T\mathbf{Q}_n + \rho_2\mathbf{Z}_i - \mathbf{\Phi}_i) \tag{14}$$

And,

$$\mathcal{M} = \arg\min_{\mathcal{M}} \|\mathcal{M}\|_{\circledast} + \frac{\rho_3}{2} \|\mathcal{M} - \mathcal{Z} + \frac{\Gamma}{\rho_3}\|_F^2. \tag{15}$$

(15) can be solved by Tensor Singular Value Convoluting (TSVC) [15] using t-SVD. And,

$$\begin{aligned} \min_{\mathcal{Z}} \quad & \sum_{i=1}^{3} \beta_i \cdot \left(\frac{\rho_2}{2} \|\mathbf{R}_i - \mathbf{Z}_{(i)} + \frac{\mathbf{\Phi}_i}{\rho_2}\|_F^2 \right) \\ & + \frac{\rho_3}{2} \|\mathcal{M} - \mathcal{Z} + \frac{\Gamma}{\rho_3}\|_F^2, \\ \text{s.t.} \quad & [\mathcal{Z}]_\Omega = [\mathcal{X}]_\Omega, \end{aligned} \tag{16}$$

The update formulae of $\mathcal{Z}$ are computed as:

$$[\mathcal{Z}]_\Omega = \left[\frac{\sum_{i=1}^{3} \beta_i(\text{fold}_i(\mathbf{\Phi}_i + \rho_2\mathbf{R}_i)) + \rho_3\mathcal{M} + \Gamma}{\rho_3 + \sum_{i=1}^{3} \beta_i\rho_2} \right]_\Omega \tag{17}$$

and $[\mathcal{Z}]_\Omega = [\mathcal{Y}]_\Omega$ With these update formulae, the algorithm for (9) are summarized in Algorithm 1.

Fig. 2. Visual comparison of different methods on color image inpainting. Each row denotes the results of different methods on barbara and house with missing rates being 90%.

4. EXPERIMENTAL RESULTS

We conduct experiments of the RGB-color images recovery to demonstrate the effectiveness of the proposed algorithms. We compare with four state-of-the-art LRTC algorithms, including tucker-decomposition based algorithms, i.e., STDC [5] and LRTC-TV [4], and two t-SVD based algorithms, i.e., GTNN [15] and TRPCA [7]. The parameters in those compared methods were manually adjusted according to their default strategies. The experimental results are evaluated by the peak signal-to-noise ratio (PSNR), and the relative squared error (RSE), which are widely used in the visual data inpainting tasks.

$$\mathrm{PSNR} = 10 \log_{10} \frac{n_1 n_2 n_3 \|\mathcal{X}\|_\infty^2}{\|\mathcal{Z} - \mathcal{X}\|_F^2}, \ \mathrm{RSE} = \frac{\|\mathcal{Z} - \mathcal{X}\|_F}{\|\mathcal{X}\|_F}.$$

where $\mathcal{X}$ and $\mathcal{Z}$ represent the ground-truth tensor and the recovered tensor, respectively. $\|\mathcal{X}\|_\infty$ denotes the maximum value in the ground-truth tensor.

4.1. Color Image Inpainting

Figure 2 shows the ground-truth of eight images used for the experiment. The size of each image is $256 \times 256 \times 3$, which is represented as a 256-by-256-by-3 tensor. We randomly mask off 60%, 70%, 80%, 90% entries in each image, and regard them as missing values. We record the PSNR of the eight images, and compare the inpainting results quantitatively and visually.

Table 1 presents the performance of all the compared methods. From Table 1, we can see that: (i) our model outperforms other algorithms in all the cases; (ii) TV regularized algorithms, ours and LRTC-TV can recovery the color images better than those without TV regularization; (iii) TNN norm can more efficient exploit the low-rank structures of the color images, since TNN based algorithms, i.e., TRPCA and GTNN works better than STDC.

Table 1. Average performance evaluation on 8 color images with MPSNR (dB) and MSSIM.

Ratio	Metrics	STDC	LRTC-TV	TRPCA	GTNN	Ours
0.4	PSNR	25.84	28.49	27.64	27.48	**29.10**
	RSE	0.0938	0.0683	0.0768	0.0782	**0.0644**
0.3	PSNR	24.38	26.65	25.40	25.18	**27.28**
	RSE	0.1105	0.0838	0.0989	0.1013	**0.0788**
0.2	PSNR	22.75	24.49	22.80	22.73	**25.11**
	RSE	0.1327	0.1065	0.1325	0.1338	**0.0999**
0.1	PSNR	19.90	21.12	18.90	19.38	**21.87**
	RSE	0.1827	0.1561	0.2063	0.1955	**0.1435**

To make a further investigation and comparison, we visualize the recovered results of some examples in Figure 2 We can see that, with the total variation constraint, both our method and LRTC-TV obtain more clear objects and smoother pictures.

5. CONCLUSIONS

In this paper, we present a novel TV regularized tensor low-rank method based on tensor nuclear norm for color image recovery. In our model, the tensor nuclear norm is utilized to describe the global spatial-and-channel correlation, and an anisotropic spatial-spectral total variation regularization is designed to characterize the piecewise smooth structure in the spatial domain. The effectiveness of the proposed algorithm are demonstrated by color image inpainting task, and the advantages of TNN and TV regularization are explicitly shown.

Acknowledgements

The research was supported by NSFC (No. 61671290), the Key Program for International S&T Cooperation Project of China (No. 2016YFE0129500), and Shanghai Committee of Science and Technology (No. 17511101903).

References

[1] Chengcheng Jia, Guoqiang Zhong, and Yun Raymond Fu, "Low-rank tensor learning with discriminant analysis for action classification and image recovery.," in *AAAI*, 2014, pp. 1228–1234.

[2] Donald Goldfarb and Zhiwei Qin, "Robust low-rank tensor recovery: Models and algorithms," *SIAM Journal on Matrix Analysis and Applications*, vol. 35, no. 1, pp. 225–253, 2014.

[3] Tamara G Kolda and Jimeng Sun, "Scalable tensor decompositions for multi-aspect data mining," in *Data Mining, 2008. ICDM'08. Eighth IEEE International Conference on*. IEEE, 2008, pp. 363–372.

[4] Xutao Li, Yunming Ye, and Xiaofei Xu, "Low-rank tensor completion with total variation for visual data inpainting.," in *AAAI*, 2017, pp. 2210–2216.

[5] Qibin Zhao, Liqing Zhang, and Andrzej Cichocki, "Bayesian cp factorization of incomplete tensors with automatic rank determination," *IEEE transactions on pattern analysis and machine intelligence*, vol. 37, no. 9, pp. 1751–1763, 2015.

[6] Wenrui Hu, Dacheng Tao, Wensheng Zhang, Yuan Xie, and Yehui Yang, "The twist tensor nuclear norm for video completion," *IEEE transactions on neural networks and learning systems*, 2016.

[7] Canyi Lu, Jiashi Feng, Yudong Chen, Wei Liu, Zhouchen Lin, and Shuicheng Yan, "Tensor robust principal component analysis: Exact recovery of corrupted low-rank tensors via convex optimization," in *Proceedings of the IEEE Conference on Computer Vision and Pattern Recognition*, 2016, pp. 5249–5257.

[8] Pan Zhou, Canyi Lu, Zhouchen Lin, and Chao Zhang, "Tensor factorization for low-rank tensor completion," *IEEE Transactions on Image Processing*, 2017.

[9] Xiao-Yang Liu, Shuchin Aeron, Vaneet Aggarwal, and Xiaodong Wang, "Low-tubal-rank tensor completion using alternating minimization," *arXiv preprint arXiv:1610.01690*, 2016.

[10] J Douglas Carroll and Jih-Jie Chang, "Analysis of individual differences in multidimensional scaling via an N-way generalization of eckart-young decomposition," *Psychometrika*, vol. 35, no. 3, pp. 283–319, 1970.

[11] Christopher J Hillar and Lek-Heng Lim, "Most tensor problems are NP-hard," *Journal of the ACM (JACM)*, vol. 60, no. 6, pp. 45, 2013.

[12] Joseph M Landsberg, *Tensors: geometry and applications*, vol. 128, American Mathematical Society Providence, RI, 2012.

[13] M.E. Kilmer, K. Braman, N. Hao, and R.C. Hoover, "Third-order tensors as operators on matrices: A theoretical and computational framework with applications in imaging," *SIAM Journal on Matrix Analysis and Applications*, vol. 34, no. 1, pp. 148–172, 2013.

[14] Wei He, Hongyan Zhang, Liangpei Zhang, and Huanfeng Shen, "Total-variation-regularized low-rank matrix factorization for hyperspectral image restoration," *IEEE Transactions on Geoscience and Remote Sensing*, vol. 54, no. 1, pp. 178–188, 2016.

[15] Zemin Zhang, Gregory Ely, Shuchin Aeron, Ning Hao, and Misha Kilmer, "Novel methods for multilinear data completion and de-noising based on tensor-SVD," in *Proceedings of the IEEE Conference on Computer Vision and Pattern Recognition*, 2014, pp. 3842–3849.

[16] Ji Liu, Przemyslaw Musialski, Peter Wonka, and Jieping Ye, "Tensor completion for estimating missing values in visual data," *IEEE Transactions on Pattern Analysis and Machine Intelligence*, vol. 35, no. 1, pp. 208–220, 2013.